LETTER

Hydraulic diversity of forests regulates ecosystem resilience during drought

William R. L. Anderegg[1]*, Alexandra G. Konings[2], Anna T. Trugman[1], Kailiang Yu[1], David R. Bowling[1], Robert Gabbitas[1], Daniel S. Karp[3], Stephen Pacala[4], John S. Sperry[1], Benjamin N. Sulman[5,6] & Nicole Zenes[1]

Plants influence the atmosphere through fluxes of carbon, water and energy[1], and can intensify drought through land–atmosphere feedback effects[2–4]. The diversity of plant functional traits in forests, especially physiological traits related to water (hydraulic) transport, may have a critical role in land–atmosphere feedback, particularly during drought. Here we combine 352 site-years of eddy covariance measurements from 40 forest sites, remote-sensing observations of plant water content and plant functional-trait data to test whether the diversity in plant traits affects the response of the ecosystem to drought. We find evidence that higher hydraulic diversity buffers variation in ecosystem flux during dry periods across temperate and boreal forests. Hydraulic traits were the predominant significant predictors of cross-site patterns in drought response. By contrast, standard leaf and wood traits, such as specific leaf area and wood density, had little explanatory power. Our results demonstrate that diversity in the hydraulic traits of trees mediates ecosystem resilience to drought and is likely to have an important role in future ecosystem–atmosphere feedback effects in a changing climate.

Water, carbon and energy exchanges from the land surface strongly influence the atmosphere and climate; these exchanges are dominated by plants in most ecosystems[1]. Plant physiological responses to water stress influence these fluxes[5,6], and the resulting land-surface feedback effects influence local weather as well as the regional atmospheric circulation[7]. Furthermore, changes in vegetation physiology and cover can drive shifts in sensible and latent heat fluxes that intensify droughts[2–4,8]. Anthropogenic climate change is expected to intensify the hydrological cycle globally, leading to more frequent and more severe droughts in many regions[9]. Therefore, understanding the drivers of land–atmosphere feedback effects during drought and simulating them in Earth system models is critical for robust future projections and assessment of climate change impacts.

Seminal work has shown that grassland plots with more species exhibit smaller declines in productivity during drought and recover productivity much faster following drought[10], indicating that plant biodiversity—particularly functional diversity—may be important for capturing how the land surface interacts with the atmosphere during extreme events. Indeed, it is well-established that—just as a diversified stock portfolio is more likely to survive market turbulence[11]—diversity can stabilize community function through multiple mechanisms[12]. First, diverse communities are more likely to contain species with different traits that dictate how they respond to disturbances[13]. As a result, at least some species are likely to persist through any given disturbance[14]. Second, diverse communities are more likely to contain competitors that exhibit compensatory dynamics: when drought causes one species to decline in function, its competitor may increase in function and stabilize community function[12]. Critically, diversity–stability effects are mostly absent in most global land-surface models, most of which represent each biome or plant functional type with a single set of functional traits[15], partly owing to a lack of understanding of which functional traits are the most important at ecosystem scales.

Diversity in the water transport strategies of plants has been hypothesized to play a critical part in regulating the response of an ecosystem to drought[16,17]. Plant water transport through the hydraulic continuum is mediated by a variety of traits[18,19], including xylem vulnerability to embolism, stomatal regulation and other characteristics[20]. Thus, diversity of plant hydraulic strategies and traits could buffer an ecosystem against drought, as some species will curtail gas exchange and latent heat flux through transpiration before others. However, the physiological mechanisms that govern water transport through the hydraulic continuum do not correspond well with traditional plant functional types in land-surface models[21,22]. This raises the prospect that land-surface models may be missing a critical component of functional diversity when simulating future climate scenarios with a more intense hydrological cycle.

Here we test whether plant trait diversity in forests can directly affect land–atmosphere interactions by mediating and buffering the response of latent heat fluxes to changes in water availability. We combine climate data, 352 site-years of eddy covariance data from 40 temperate and boreal forest sites across the globe (Extended Data Fig. 1 and Supplementary Table 1), and datasets of multiple plant functional traits at the species level. We test which site-level factors (for example, stand age) and plant traits are most associated with ecosystem flux variation in response to drought and whether diversity in response traits stabilizes fluctuations in ecosystem fluxes during drought periods.

We first examine which plant traits and site-level factors can best predict how eddy covariance measurements of daily latent energy exchange (a proxy for forest transpiration) vary in response to water availability. At each eddy covariance site, we quantified this drought response with two complementary metrics: the 'drought coupling' (model R^2) and the 'drought sensitivity' (standardized model coefficient values) of a multiple regression of latent energy as a function of vapour pressure deficit (VPD), soil moisture and their interaction (equation (1) in the Methods). All else being equal, forest sites with lower coupling and lower sensitivity will experience smaller variation (higher resilience) in latent energy fluxes explained by variations in VPD and soil moisture.

We considered site factors—stand age, species richness and gymnosperm fraction—and the mean and standard deviation of key functional traits expected to influence drought responses. We examined wood density, specific leaf area, maximum light-saturated photosynthetic rate (A_{max}), the water potential at which 50% of stem xylem conductivity is lost (P_{50}), the minimum stem water potential typically experienced (Psi_{min}) and several estimates of the hydraulic safety margin[18,23] (HSM; the difference between Psi_{min} and P_{50} in Fig. 1; alternative analyses in Supplementary Table 2). We compiled trait data for the dominant tree species at each site that make up more than 80% of the biomass (mean trait coverage: 91% of biomass). A strong influence of mean trait values indicates the importance of particular trait values in dictating community-wide responses to drought. By contrast, the influence of trait standard deviations suggests that it is the trait diversity per se that buffers communities[24]. We used univariate regression with

[1]School of Biological Sciences, University of Utah, Salt Lake City, UT, USA. [2]Department of Earth System Science, Stanford University, Stanford, CA, USA. [3]Department of Wildlife, Fish, and Conservation Biology, University of California, Davis, Davis, CA, USA. [4]Department of Ecology and Evolutionary Biology, Princeton University, Princeton, NJ, USA. [5]Program in Atmospheric and Oceanic Sciences, Princeton University, Princeton, NJ, USA. [6]School of Natural Sciences, University of California, Merced, Merced, CA, USA. *e-mail: anderegg@utah.edu
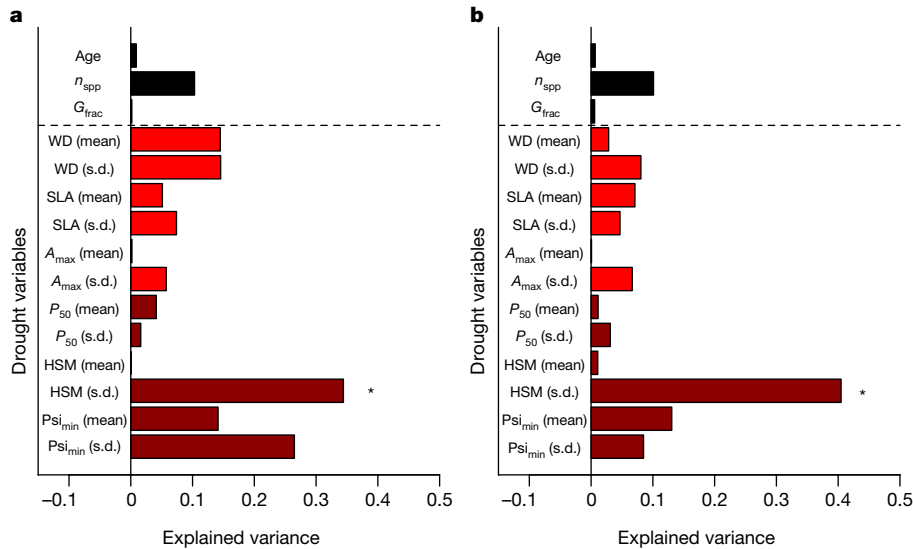
Fig. 1 | Variation in hydraulic traits mediates ecosystem flux response to drought. The percentage of explained variance (R^2) in an ordinary least-squares linear regression of community-weighted plant traits (dark red, hydraulic traits; red, other traits) and site metrics (black, above the dashed line) in explaining cross-site patterns in the coupling (**a**) and sensitivity (**b**) of latent energy exchange variation in response to drought variables. Site metrics include: forest age (Age), species richness (n_{spp}) and fraction of forest composition that is gymnosperm species (G_{frac}). Traits include the community-weighted mean and standard deviation (s.d.) of: wood density (WD), specific leaf area (SLA), A_{max}, P_{50}, HSM and Psi_{min}. For samples sizes for each trait, see Supplementary Table 3. Asterisks indicate statistically significant regressions ($P = 0.001$ (**a**) and $P = 0.02$ (**b**) after correction for multiple hypothesis testing).

individual traits, multivariate regression with model selection using the Akaike information criterion (AIC) and a machine-learning algorithm (random forests) to identify the most critical traits or site factors.

Of the tested traits, the community-level variation in HSM was the most predictive of forest flux responses to drought (Fig. 1), explaining 41% and 34% of the cross-site patterns in univariate models of drought coupling and drought sensitivity, respectively ($P < 0.01$ and $P = 0.02$ after correction for multiple hypothesis testing). However, considerable variation in drought coupling and sensitivity existed at sites where the HSM variation was low. Model selection techniques on multivariate trait models showed that the standard deviation of HSM and mean maximum photosynthetic rate were the most parsimonious models for drought sensitivity ($R^2 = 0.45$, $P < 0.001$, ΔAIC < -2 from all other models). The standard deviation of HSM alone was selected as the most parsimonious model for drought coupling ($R^2 = 0.41$, $P = 0.001$). Model selection further indicated that the remaining predictors had little effect on model performance. In addition, the machine-learning algorithm consistently indicated that the standard deviation of HSM was one of the most important predictor variables (Extended Data Fig. 2).

We found that higher diversity in the HSMs of the species in an ecosystem significantly buffers ecosystem latent heat flux response to drought ($P_{sens} = 0.003$, $P_{coup} = 0.001$; Fig. 2). All else being equal, forest communities with higher hydraulic diversity (defined as a higher standard deviation in HSM) experienced smaller variation in latent energy fluxes explained by VPD and soil moisture. This pattern was generally robust, especially for the drought coupling metric, to the method of data processing including: (1) adjustment of measured latent energy exchange to correct for energy balance non-closure ($P_{coup} = 0.007$); (2) using both standardized (z-score) and raw drought variables ($P_{coup} = 0.001$); (3) alternative estimates of the HSM (Supplementary Table 2 and Extended Data Fig. 3); and (4) accounting for other potentially confounding factors such as forest age (Methods).

We found here that plant trait variation, particularly hydraulic diversity, has a critical role in the response of temperate and boreal forests to drought. The importance of trait variation metrics (Fig. 1), as opposed to trait mean metrics, highlights a critical role of compensatory dynamics among species in how functional diversity mediates ecosystem responses to climate extremes (Supplementary Information). We acknowledge, however, that our analysis is limited to 40 flux sites

and the examined traits do not capture all the important elements of the drought-response strategies of each species. More traits, particularly rooting depth and allometric differences (for example, leaf-to-sapwood ratios), will probably help to explain some of the remaining variations in ecosystem resilience. Furthermore, our sites generally do not include droughts that are severe enough to trigger tree mortality or changes in species composition, which may be important processes that influence the long-term response of an ecosystem to drought[25].

Recent advances have shown that plant hydraulics can be used to predict stomatal responses to changing environmental conditions[19,26] and the simulation of plant hydraulic transport in Earth-system models
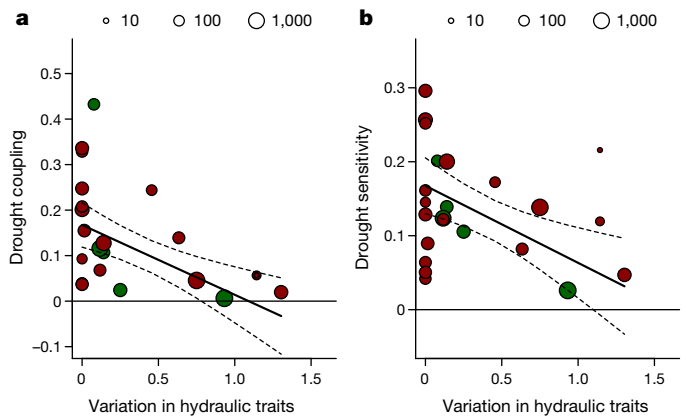

Fig. 2 | Ecosystem sensitivity to drought as a function of community variation in hydraulic safety margin. a, Drought coupling is expressed as the percentage of explained variation (R^2). **b**, Drought sensitivity is expressed as the summed absolute values of standardized coefficients of drought variables regressed against latent energy (LE) exchange as a function of daily VPD, soil moisture (SM) and their interaction (regression: LE = f(VPD, SM, VPD × SM)). Hydraulic variation is expressed as the community-weighted standard deviation in the HSM of each species. Colours indicate biomes of deciduous broadleaf (green) and needleleaf (red) forests. The size of the dot indicates the number of days included for each flux site. The solid black line is the best-fit ordinary least-squares linear regression and dashed lines are the 95% confidence interval of the regression fit ($n = 23$ independent sites).
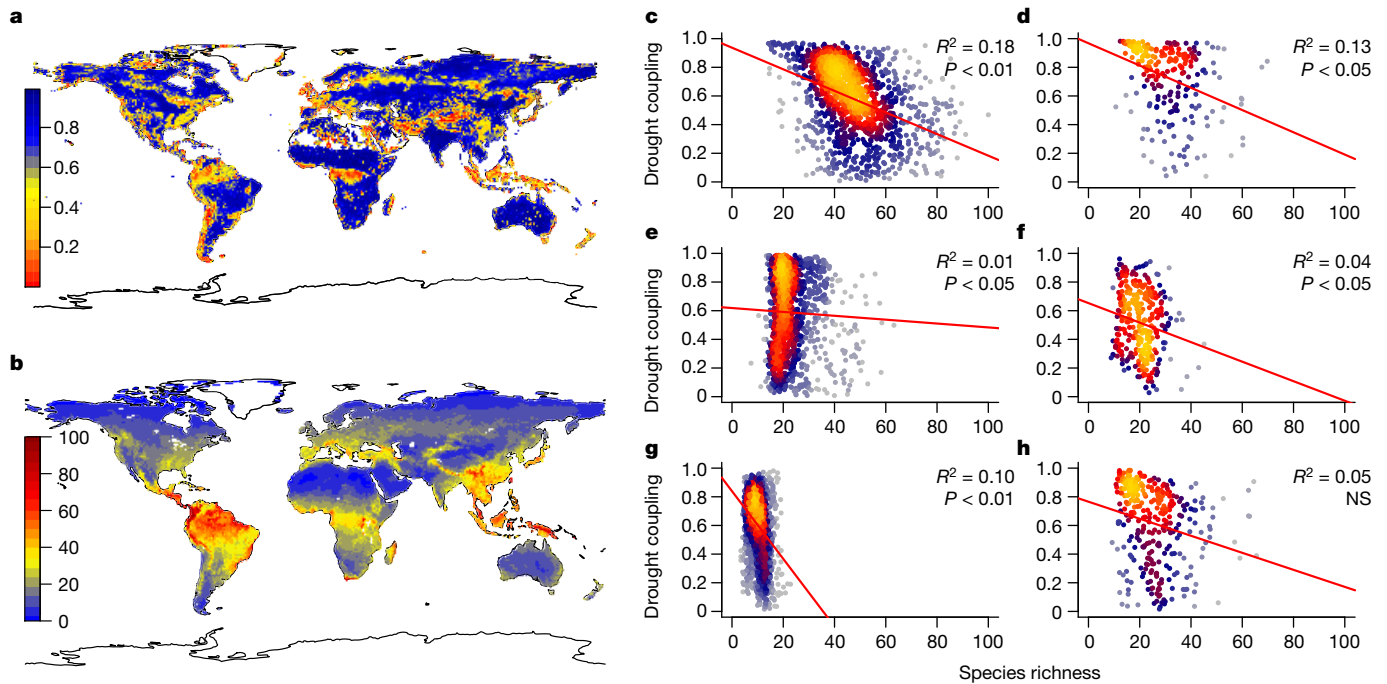
Fig. 3 | Forest ecosystem response to drought estimated from remote-sensing-derived vegetation water content variation is influenced by species richness. a, Drought coupling as the percentage of explained variation (R^2) in an ordinary least-squares linear regression by drought variables on an index of aboveground plant water content variation at midday (regression: vegetation optical depth at midday (VOD_{midday}) = $f(VOD_{night}, VPD)$). **b**, Native plant species richness (percentage of the maximum). Data available from http://ecotope.org/anthromes/biodiversity/plants/data/. **c–h**, Regressions between these two variables for six major biomes. **c**, Tropical and subtropical moist broadleaf forests.

$n = 1,380$ grid cells. **d**, Tropical and subtropical dry broadleaf forests. $n = 241$ grid cells. **e**, Temperate broadleaf and mixed forests. $n = 1,289$ grid cells. **f**, Temperate coniferous forests. $n = 318$ grid cells. **g**, Boreal forests. $n = 1,784$ grid cells. **h**, Mediterranean-type forests, woodlands and shrubs. $n = 319$ grid cells. Each point represents an individual grid cell from the map and redder colours indicate a higher density of points. Red lines show ordinary least-squares regression lines of best fit. Numbers in the upper right of panels indicate the linear generalized least-squares regression R^2 and P values indicate statistical significance of that regression after accounting for spatial autocorrelation.

is now possible[27]. Current land-surface models largely do not simulate diversity in strategies in plant response to drought, nor do they currently include plant hydraulics, potentially leading to substantial carbon cycle uncertainty[28]. Efforts are underway to develop and test functional trait-based models at the Earth-system scale[15]. Incorporating plant hydraulic diversity, especially through diversity in P_{50} and stomatal response to water potential (for example, HSM), will also improve the representation of related processes. For example, the loss of plant hydraulic transport is the key mechanism of drought-induced mortality[29] and can predict mortality risk among species in diverse communities[30].

Our broadly distributed temperate and boreal forest flux tower analyses suggest that drought resilience signals from biodiversity might be observable in satellite-based estimates of vegetation water content (Methods and Extended Data Figs. 4, 5). As a preliminary exploration, we examined covariation of the variability in vegetation water content with dominant tree species diversity across the continental United States and conducted a similar, more speculative analysis at global scales. Similar to the eddy flux tower findings, higher species diversity was associated with a more buffered response of vegetation water content to drought indicators across the United States ($P_{sens} = 0.0005$; $P_{coup} < 0.0001$; Extended Data Fig. 6) and globally within tropical moist ($P < 0.0001$), tropical dry ($P = 0.03$), temperate broadleaf ($P = 0.01$), temperate conifer ($P = 0.02$) and boreal ($P < 0.0001$) forest ecosystems, and was marginally associated in Mediterranean-type woodlands ($P = 0.07$) (Fig. 3 and Extended Data Fig. 7). Species richness was also an important predictor variable identified using the machine-learning algorithm (Extended Data Fig. 8), for which the complete model explained 27% of the variance in drought responses in global forests. The influence of diversity on ecosystem sensitivity showed strong biome-specific differences (Fig. 3). Across biomes, we observed a saturating relationship between the biodiversity and drought sensitivity of the ecosystems (Extended Data Fig. 9), although this appears to be driven by biome-level

differences in sensitivity. Although this initial exploration should be treated with caution before a more detailed observational validation is performed, it provides a starting point for global analyses of how forest diversity regulates ecosystem resilience during drought that is consistent with conclusions drawn from flux tower analysis.

We have documented a fundamental effect of trait variation on ecosystem stability that directly influences the atmosphere and climate system. Temperate and boreal forest ecosystems with higher hydraulic diversity are more buffered to changing drought conditions. Owing to the paucity of eddy covariance sites and physiological trait measurements at tropical forest sites, additional measurements are needed to test these diversity–stability patterns in more diverse forests. Our initial analysis suggests that satellite measurements of canopy water content may be promising for overcoming some of the scarcity barrier of limited eddy covariance sites for scaling and testing drought responses at continental scales. Our results provide evidence that hydraulic diversity is a critical element of biodiversity for next-generation land-surface models to include to improve simulations of carbon, water and energy fluxes in a rapidly changing climate.

Online content

Any methods, additional references, Nature Research reporting summaries, source data, statements of data availability and associated accession codes are available at https://doi.org/10.1038/s41586-018-0539-7.

1. Bonan, G. B. Forests and climate change: forcings, feedbacks, and the climate benefits of forests. *Science* **320**, 1444–1449 (2008).
2. Seneviratne, S. I. et al. Impact of soil moisture–climate feedbacks on CMIP5 projections: first results from the GLACE-CMIP5 experiment. *Geophys. Res. Lett.* **40**, 5212–5217 (2013).

3. Berg, A. et al. Land–atmosphere feedbacks amplify aridity increase over land under global warming. *Nat. Clim. Change* **6**, 869–874 (2016).
4. Dirmeyer, P. A. Vegetation stress as a feedback mechanism in midlatitude drought. *J. Clim.* **7**, 1463–1483 (1994).
5. Sulman, B. N. et al. High atmospheric demand for water can limit forest carbon uptake and transpiration as severely as dry soil. *Geophys. Res. Lett.* **43**, 9686–9695 (2016).
6. Novick, K. A. et al. The increasing importance of atmospheric demand for ecosystem water and carbon fluxes. *Nat. Clim. Change* **6**, 1023–1027 (2016).
7. Khanna, J., Medvigy, D., Fueglistaler, S. & Walko, R. Regional dry-season climate changes due to three decades of Amazonian deforestation. *Nat. Clim. Change* **7**, 200–204 (2017).
8. Teuling, A. J. et al. Contrasting response of European forest and grassland energy exchange to heatwaves. *Nat. Geosci.* **3**, 722–727 (2010).
9. IPCC. *Managing the Risks of Extreme Events and Disasters to Advance Climate Change Adaptation. A Special Report of Working Groups I and II of the Intergovernmental Panel on Climate Change.* (Cambridge Univ. Press, Cambridge, 2012).
10. Tilman, D., Wedin, D. & Knops, J. Productivity and sustainability influenced by biodiversity in grassland ecosystems. *Nature* **379**, 718–720 (1996).
11. Doak, D. F. et al. The statistical inevitability of stability–diversity relationships in community ecology. *Am. Nat.* **151**, 264–276 (1998).
12. Tilman, D., Isbell, F. & Cowles, J. M. Biodiversity and ecosystem functioning. *Annu. Rev. Ecol. Evol. Syst.* **45**, 471–493 (2014).
13. Naeem, S. & Wright, J. P. Disentangling biodiversity effects on ecosystem functioning: deriving solutions to a seemingly insurmountable problem. *Ecol. Lett.* **6**, 567–579 (2003).
14. Mori, A. S., Furukawa, T. & Sasaki, T. Response diversity determines the resilience of ecosystems to environmental change. *Biol. Rev. Camb. Philos. Soc.* **88**, 349–364 (2013).
15. Scheiter, S., Langan, L. & Higgins, S. I. Next-generation dynamic global vegetation models: learning from community ecology. *New Phytol.* **198**, 957–969 (2013).
16. Matheny, A. M., Mirfenderesgi, G. & Bohrer, G. Trait-based representation of hydrological functional properties of plants in weather and ecosystem models. *Plant Divers.* **39**, 1–12 (2017).
17. Anderegg, W. R. L. et al. Woody plants optimise stomatal behaviour relative to hydraulic risk. *Ecol. Lett.* **21**, 968–977 (2018).
18. Choat, B. et al. Global convergence in the vulnerability of forests to drought. *Nature* **491**, 752–755 (2012).
19. Sperry, J. S. et al. Pragmatic hydraulic theory predicts stomatal responses to climatic water deficits. *New Phytol.* **212**, 577–589 (2016).
20. Brodribb, T. J. Xylem hydraulic physiology: the functional backbone of terrestrial plant productivity. *Plant Sci.* **177**, 245–251 (2009).
21. Anderegg, W. R. Spatial and temporal variation in plant hydraulic traits and their relevance for climate change impacts on vegetation. *New Phytol.* **205**, 1008–1014 (2015).
22. Konings, A. G. & Gentine, P. Global variations in ecosystem-scale isohydricity. *Glob. Change Biol.* **23**, 891–905 (2017).
23. Martin-StPaul, N., Delzon, S. & Cochard, H. Plant resistance to drought depends on timely stomatal closure. *Ecol. Lett.* **20**, 1437–1447 (2017).
24. Suding, K. N. et al. Scaling environmental change through the community-level: a trait-based response-and-effect framework for plants. *Glob. Change Biol.* **14**, 1125–1140 (2008).
25. Zhang, T., Niinemets, Ü., Sheffield, J. & Lichstein, J. W. Shifts in tree functional composition amplify the response of forest biomass to climate. *Nature* **556**, 99–102 (2018).
26. Wolf, A., Anderegg, W. R. L. & Pacala, S. W. Optimal stomatal behavior with competition for water and risk of hydraulic impairment. *Proc. Natl Acad. Sci. USA* **113**, E7222–E7230 (2016).
27. Bonan, G. B., Williams, M., Fisher, R. A. & Oleson, K. W. Modeling stomatal conductance in the earth system: linking leaf water-use efficiency and water transport along the soil–plant–atmosphere continuum. *Geosci. Model Dev.* **7**, 2193–2222 (2014).
28. Trugman, A., Medvigy, D., Mankin, J. & Anderegg, W. R. L. Soil moisture stress as a major driver of carbon cycle uncertainty. *Geophys. Res. Lett.* **45**, 6495–6503 (2018).
29. Nardini, A., Battistuzzo, M. & Savi, T. Shoot desiccation and hydraulic failure in temperate woody angiosperms during an extreme summer drought. *New Phytol.* **200**, 322–329 (2013).
30. Anderegg, W. R. L. et al. Meta-analysis reveals that hydraulic traits explain cross-species patterns of drought-induced tree mortality across the globe. *Proc. Natl Acad. Sci. USA* **113**, 5024–5029 (2016).

METHODS

Flux tower analysis. We used the FLUXNET2015 Tier 1 dataset of eddy covariance sites (http://fluxnet.fluxdata.org/data/fluxnet2015-dataset/) around the world to quantify ecosystem sensitivity to drought and the degree to which plant traits mediate ecosystem flux variation due to changes in environmental drivers. The FLUXNET2015 dataset provides a standardized set of fluxes of carbon, water and energy at over 210 sites and has undergone a standard set of quality assurance and quality control tests and gap-filling[31]. Using the biome classification from the International Geosphere–Biosphere Programme (IGBP) provided for the FLUXNET2015 sites, we selected sites that were forest or woodland ecosystems (deciduous broadleaf forest, evergreen needleleaf forest, evergreen broadleaf forest or mixed forest) and sites that had not experienced disturbance in at least 10 years before flux monitoring, to avoid sites with frequent disturbances or rapidly developing vegetation. This led to a list of 65 candidate sites. Because adequate on-site climate data are needed to determine drought sensitivity and knowledge of the functional traits of dominant canopy species, we further excluded sites that did not have on-site measurements of the vapour pressure saturation deficit of air (VPD, calculated from temperature and relative humidity and reported as a derived variable in the FLUXNET2015 dataset), soil water content of the top 30 cm, or sites that did not have adequate species coverage of functional trait measurements (see below) for at least two of our functional traits. This led to a final site list of 40 forest sites around the world (Supplementary Table 1 and Extended Data Fig. 1), covering 352 site-years of data.

We used a previously published method[5] that was specifically designed to estimate drought sensitivity at a given eddy covariance site by focusing on days when water availability was most likely to control ecosystem fluxes (for example, screening out days when other meteorological drivers, such as radiation, were likely to be more important influences on fluxes). In brief, we used the daily-level records of latent energy exchange as dependent variables to quantify variation in water and energy fluxes. Latent energy is dominated by plant transpiration in forest ecosystems under certain conditions[5,6] and thus variation in latent energy exchange is a major mechanism through which plants on the land surface affect the atmosphere. Following previous analyses[5], we conservatively selected only days on which latent heat was dominated by transpiration, changes in leaf area were likely to be relatively minor, and flux variation was likely to be influenced by water availability. Thus, at each site, we restricted our analysis to days during the peak of growing season, quantified as days on which: (1) the average temperature was above 15 °C; (2) solar radiation was high, quantified as days in which 24-h average photosynthetic photon flux density was greater than 500 μmol m^{-2} s^{-1}; and (3) sufficient evaporative demand existed to drive water fluxes, quantified as 24-h average VPD > 0.5 kPa. For all analyses, we used both the 'LE' and 'LE.CORR' variables reported by the FLUXNET2015 database for latent energy exchange. LE.CORR reflects a correction factor, which assumes that the measured Bowen ratio is correct; this factor scales the energy fluxes with the measured Bowen ratio and is used to force energy balance closure at each flux site. Our results were robust to either variable. Following previous analyses[5], we standardized the timeseries of latent energy by dividing by the mean latent energy at a given site where VPD was between 0.9 and 1.1 kPa and volumetric soil water content was >90th percentile (considered to be well-hydrated conditions). This standardization allowed for cross-site comparison of latent energy sensitivity to climate conditions, by accounting for fixed extrinsic (for example, stand biomass or leaf area) drivers.

Once this subset of days was determined, we constructed a multivariate drought model for each site by performing a multiple linear regression of daily latent energy exchange (LE) as a function of daily VPD, soil moisture (SM) and their interaction, as has previously been done for cross-site comparisons in eddy covariance data[5,6]:

$$LE = \beta_1 VPD + \beta_2 SM + \beta_3 SM \times VPD + \varepsilon \qquad (1)$$

in which β_i indicates the regression coefficient for term i. Consistent with previous drought regression studies that focused on temperate forest eddy covariance sites across the United States[5,6], soil moisture in the top 30 cm was used because data for soil moisture from deeper layers are rarely available. We note that soil moisture is challenging to quantify across flux sites and absolute values of volumetric water content of soil should be treated with caution. This multivariate regression method has been used successfully in multiple temperate forest studies across the United States to quantify the sensitivity of ecosystems to the critical components of drought stress[5,6] and performed relatively well at our flux sites (Extended Data Fig. 10).

The adjusted R^2 values of these regressions represent the degree to which ecosystem-level variation in latent energy exchange was controlled by VPD and soil moisture and was subsequently used as a dependent variable ('drought coupling' in the main text) in our cross-site analysis. In addition, we further performed all multiple linear regressions with standardized (z-score) VPD, soil moisture and their interaction, which enabled quantitative comparison of the regression

coefficients[32]. We summed the absolute values of the three coefficients to provide a metric of 'drought sensitivity' at each flux site.

From published literature, we compiled the species composition and, where possible, dominance of tree species at each flux site (Supplementary Tables 3, 4). Using a combination of the metadata and studies listed on the host site for each flux tower and targeted literature searches, we created a database of the dominant tree species in the footprint of each flux tower. For 22 of the 40 sites (Supplementary Tables 3, 4), we were able to acquire estimates of relative dominance of each species, typically through metrics of basal area or composition percentage, and we converted these metrics to the proportion of each species within the total plant community (that is, between 0 and 1). These values were used in a subsequent analysis to calculate community-weighted (for example, dominance-weighted) trait means and standard deviations.

Trait analysis. We compiled trait data for dominant tree species that comprised >80% of the biomass and/or composition at all sites (mean across all sites: 91%), which enabled capturing first-order effects of functional traits on ecosystem water fluxes. For sites for which biomass and/or composition data were not available, we assumed that all 'dominant' species listed in the publication had equal composition. We used the Global Wood Density Database[33,34] to compile wood density data for species. We used a previously published dataset[35] to compile the traits of each species for light-saturated maximum photosynthetic rate and specific leaf area (SLA). Traits related to photosynthetic rates and SLA are prominent traits that are typically considered as inputs for next-generation 'trait-based' models, and SLA is often related to leaf metabolic rates and lifespan in these models. We used the Xylem Functional Traits database[36] to compile the water potential at 50% loss of hydraulic conductivity (P_{50}) and the HSM, defined as the difference between P_{50} and the minimum water potential experienced (see alternative definitions in Supplementary Table 2), for each species. The HSM has previously been observed to be a critical predictive trait[18], because it provides an integrative assessment of species 'riskiness' during drought, integrating both hydraulic vulnerability to water potential and stomatal responses[23] and/or potentially diversity in the rooting strategies of each species. We then calculated the mean and standard deviation of each trait for each site as the community-weighted mean and standard deviation. Supplementary Table 3 describes the proportion of species composition at each site for which we had adequate trait data and sites were dropped from trait-level analyses if they had insufficient trait data.

Using the drought correlation and drought sensitivity of flux sites as dependent variables, we used three complementary approaches to determine which site factors and functional traits were most important. First, we performed univariate ordinary least-squares regressions between functional traits and the drought response metrics (Fig. 1). Because this involved multiple hypothesis testing, we implemented the Bonferroni correction to adjust P values for multiple comparisons. Because the hydraulic trait P_{50} can be sensitive to method artefacts, we repeated this analysis with alternative values for the few ($n =$ around 6–8) potentially problematic species (Supplementary Table 5) and observed that our results were robust. Second, we used models of multiple traits, determining the most parsimonious model through model selection procedures. Because variable importance estimates can be biased by collinear predictor variables, we used a matrix of pairwise correlations and removed any variable with high correlations ($R > 0.5$) with other predictor variables. Each pairwise correlation was performed and the variable with the lower correlation with the dependent variable was removed[37]. With this reduced set of predictor variables, we then used both forward and backward stepwise model selection via AIC, with ΔAIC values of < -2 used as a criterion to drop variables[38]. This technique provides a rigorous estimate of the most parsimonious model, and the coefficients of the (previously standardized to z-score) predictor variables that remain can be compared directly. Because the quantity of data available across sites was highly variable (range 10–1,200 days that met the above criterion) and thus the variable statistical insight that can be drawn from each site varied based on this sample size (that is, a regression that covers 20 days should be down-weighted relative to a regression that covers 800 days), we weighted each site by the number of days for which data were available. For plotting Fig. 2, one site with adequate HSM data was classified 'mixed forest' by the FLUXNET2015 database and for simplicity we plotted it as an 'evergreen needleleaf forest', because it was dominated by gymnosperm species.

Finally, we used a machine-learning algorithm of random forests[39] to estimate the variable importance on the non-collinear traits identified as above. We chose this algorithm because it (1) performs well among machine-learning algorithms; (2) makes no assumptions about the distribution (for example, normality) of the input data; (3) makes no assumptions on the functional form of the relationship between independent and dependent variables (for example, linear, nonlinear, and so on); and (4) can handle interactions between independent variables. We examined variable importance using the total decrease in node impurities for each variable.
Satellite estimates of drought-driven variation in vegetation water content. We tested spatial patterns of variations in drought sensitivity using ecosystem-scale

estimates of vegetation water content from microwave radiometry-derived vegetation optical depth (VOD). We used VOD from the land parameter data record, which was retrieved from the X-band (10.7 GHz) observations of the advanced microwave scanning radiometer–earth observing system (AMSR-E) based on simultaneous retrieval of atmospheric water vapour, surface soil moisture, VOD and the canopy scattering albedo. Measurements across a variety of ecosystem types have previously shown that VOD is proportional to plant water content[40] and therefore also to leaf water potential[41], although additional research is needed to determine how the relationship between VOD and plant water potential varies across ecosystems. Full retrieval algorithm details can be found in previously published studies[42–44]. Rainy days were filtered from the record to avoid contamination from intercepted water on the leaves affecting the AMSR-E observations. Data for which the land-surface temperature (derived from higher-frequencies of the AMSR-E radiometer) was below 273 K were assumed to represent frozen soil conditions for which the VOD retrieval algorithms are not valid, and were also removed from the dataset. We used data from January 2003–December 2010 (the AMSR-E failed in 2011). Rain was determined based on data from the Global Precipitation Climatology Project[45]. We compared daily midday VOD estimates to the total daily latent energy fluxes at our flux tower sites and found that the two were linearly related despite each VOD observation representing an area 2–3 orders of magnitude greater than the flux tower fetch ($P < 0.0001$, Extended Data Fig. 4), indicating that both captured the broad-scale ecosystem response to water availability. Furthermore, we observed that hydraulic diversity was correlated with tree species richness in the United States ($R^2 = 0.65$; $P = 0.04$, Extended Data Fig. 5).

To calculate drought coupling, we first conducted a similar analysis to equation (1) by calculating the R^2 for each grid cell of the regression of VOD at midday versus VOD at night and daily VPD, although without the interaction term present in equation (3). The night-time (01:30) VOD was used because it is representative of root-zone soil moisture variation, given pre-dawn equilibrium between root-zone soil water potential and leaf water potential. This R^2 was used to measure drought coupling (coefficient of determination) at global scale. To quantify drought sensitivity, we used estimates of ecosystem 'anisohydricity' derived from the same VOD data. Anisohydricity is a measure of leaf water-potential response to soil drying and increases in VPD, as influenced by stomatal closure and xylem loss of conductivity. The anisohydricity was calculated as previously published[22] based on the slope of the relationship between midday (13:30 local time) overpass VOD and midnight (01:30 local time) overpass VOD, for which—at the latter time—leaf and soil water potential are assumed to be in equilibrium owing to night-time refilling. Higher values indicate more anisohydric or less drought-sensitive ecosystems, although prolonged droughts may still lead to a reduction in growth[46].

For the US-based analysis, we used the richness of dominant tree species from a previous study[47] to compare to hydraulic diversity of our eddy covariance sites. Globally, we used the previously published dataset[48] that provides spatial patterns of plant diversity based on species-area relationships and ground plots. We converted this dataset to a raster with 1×1 degree resolution and then used the previously published biome map[49] at the same resolution to determine the biome of each grid cell. We examined only grid cells that were dominated by one of six forest biomes (moist tropical forest, dry tropical forest, broadleaf temperate forest, coniferous temperate forest, boreal forest or Mediterranean-type forest/woodland). We further screened grid cells to remove cells with >25% human impact (typically croplands) based on a previous study[50].

We converted the vegetation water content variation metrics (correlation and sensitivity to drought variables) to the same resolution using bilinear interpolation. For each biome, we examined the relationship between species richness and water content variation using linear mixed-effects models to account for spatial auto-correlation. Per standard practice[51], we included the latitude and longitude coordinates of each grid cell in the regression and tested the following spatial correlation structures—linear, quadratic ratio, exponential, spherical and Gaussian—selecting the most likely and parsimonious model using $\Delta AIC < -2$ or more. The quadratic correlation structure was most parsimonious for all biomes. We further checked that the effect of species richness was not due to patterns in biomass and/or productivity alone by including models that had both richness and the mean pixel VOD over the whole record, which is strongly related to aboveground biomass. Using stepwise model selection using AIC, the most parsimonious model included both mean VOD and species richness, indicating that richness is important beyond average biomass/productivity. Finally, we performed a similar random forest analysis and variable importance as conducted for the flux tower analysis and included species richness, mean VOD, canopy height[52] (to account for potential successional and/or land use effects) and biome.

Statistics. No statistical methods were used to predetermine sample size. All statistical analyses were performed in the R computing environment[53]. Model selection was performed using the stepAIC function in the MASS package[54]. Statistical

assumptions of linear models were verified by examining residual and quantile plots of the models and transformations were applied as needed. All maps were generated using the raster[55] and rworldmap[56] packages and spatial autocorrelation was modelled using the gls function in the nlme package[57]. The generalized additive model in Extended Data Fig. 9 was performed using the gam function in the mgcv package[58]. Random forest analyses were performed using the randomForest and ranger packages.

Reporting summary. Further information on research design is available in the Nature Research Reporting Summary linked to this paper.

Data availability

Eddy flux data are available at http://fluxnet.fluxdata.org/data/fluxnet2015-dataset/; community trait data are available at http://www.anereglab.net/data/trait-data/; detailed trait data are available in Extended Data Figs. 1–10 and at https://datadryad.org//handle/10255/dryad.235, https://datadryad.org//handle/10255/dryad.80340 and from a previous publication[18].

31. Pastorello, G. Z. et al. The FLUXNET2015 dataset: The longest record of global carbon, water, and energy fluxes is updated. *Eos* **98**, (2017).
32. Clogg, C. C., Petkova, E. & Haritou, A. Statistical methods for comparing regression coefficients between models. *Am. J. Sociol.* **100**, 1261–1293 (1995).
33. Zanne, A. E. et al. Global wood density database. *Dryad* https://doi.org/10.5061/dryad.234/1 (2009).
34. Chave, J. et al. Towards a worldwide wood economics spectrum. *Ecol. Lett.* **12**, 351–366 (2009).
35. Maire, V. et al. Global effects of soil and climate on leaf photosynthetic traits and rates. *Glob. Ecol. Biogeogr.* **24**, 706–717 (2015).
36. Gleason, S. M. et al. Weak tradeoff between xylem safety and xylem-specific hydraulic efficiency across the world's woody plant species. *New Phytol.* **209**, 123–136 (2016).
37. Anderegg, L. D. L., Anderegg, W. R. L., Abatzoglou, J., Hausladen, A. M. & Berry, J. A. Drought characteristics' role in widespread aspen forest mortality across Colorado, USA. *Glob. Change Biol.* **19**, 1526–1537 (2013).
38. Burnham, K. P. & Anderson, D. R. Multimodel inference understanding AIC and BIC in model selection. *Sociol. Methods Res.* **33**, 261–304 (2004).
39. Breiman, L. Random forests. *Mach. Learn.* **45**, 5–32 (2001).
40. Jackson, T. J. & Schmugge, T. J. Vegetation effects on the microwave emission of soils. *Remote Sens. Environ.* **36**, 203–212 (1991).
41. Momen, M. et al. Interacting effects of leaf water potential and biomass on vegetation optical depth. *J. Geophys. Res. Biogeosci.* **122**, 3031–3046 (2017).
42. Du, J., Kimball, J. S. & Jones, L. A. Passive microwave remote sensing of soil moisture based on dynamic vegetation scattering properties for AMSR-E. *IEEE Trans. Geosci. Remote Sens.* **54**, 597–608 (2016).
43. Du, J. et al. A global satellite environmental data record derived from AMSR-E and AMSR2 microwave earth observations. *Earth Syst. Sci. Data* **9**, 791–808 (2017).
44. Jones, L. A. et al. Satellite microwave remote sensing of daily land surface air temperature minima and maxima from AMSR-E. *IEEE J. Sel. Top. Appl. Earth Obs. Remote Sens.* **3**, 111–123 (2010).
45. Huffman, G. J. et al. Global precipitation at one-degree daily resolution from multisatellite observations. *J. Hydrometeorol.* **2**, 36–50 (2001).
46. Konings, A. G., Williams, A. P. & Gentine, P. Sensitivity of grassland productivity to aridity controlled by stomatal and xylem regulation. *Nat. Geosci.* **10**, 284–288 (2017).
47. Jenkins, C. N., Van Houtan, K. S., Pimm, S. L. & Sexton, J. O. US protected lands mismatch biodiversity priorities. *Proc. Natl Acad. Sci. USA* **112**, 5081–5086 (2015).
48. Ellis, E. C., Antill, E. C. & Kreft, H. All is not loss: plant biodiversity in the Anthropocene. *PLoS ONE* **7**, e30535 (2012).
49. Olson, D. M. et al. Terrestrial ecoregions of the world: a new map of life on earth: a new global map of terrestrial ecoregions provides an innovative tool for conserving biodiversity. *Bioscience* **51**, 933–938 (2001).
50. Sanderson, E. W. et al. The human footprint and the last of the wild. *Bioscience* **52**, 891–904 (2002).
51. Dormann, C. F. et al. Methods to account for spatial autocorrelation in the analysis of species distributional data: a review. *Ecography* **30**, 609–628 (2007).
52. Simard, M., Pinto, N., Fisher, J. B. & Baccini, A. Mapping forest canopy height globally with spaceborne lidar. *J. Geophys. Res.* **116**, G04021 (2011).
53. R Core Team. *R: A Language and Environment for Statistical Computing.* http://www.R-project.org/ (R Foundation for Statistical Computing, Vienna, 2012).
54. Ripley, B. et al. *MASS: Support Functions and Datasets for Venables and Ripley's MASS.* R package version 7.3-50 https://cran.r-project.org/web/packages/MASS/index.html (2013).
55. Hijmans, R. J. & van Etten, J. *raster: Geographic Data Analysis and Modeling.* R package version 2.6-7 https://cran.r-project.org/web/packages/raster/index.html (2014).
56. South, A. *rworldmap: Mapping Global Data.* R package version 1.3-6 https://cran.r-project.org/web/packages/rworldmap/index.html (2011).
57. Bates, D. et al. *lme4: Linear Mixed-Effects Models using 'Eigen' and S4.* R package version 1.1-18-1 https://cran.r-project.org/web/packages/lme4/index.html (2014).
58. Wood, S. N. mgcv: GAMs and generalized ridge regression for R. *R News* **1** (2), 20–25 (2001).
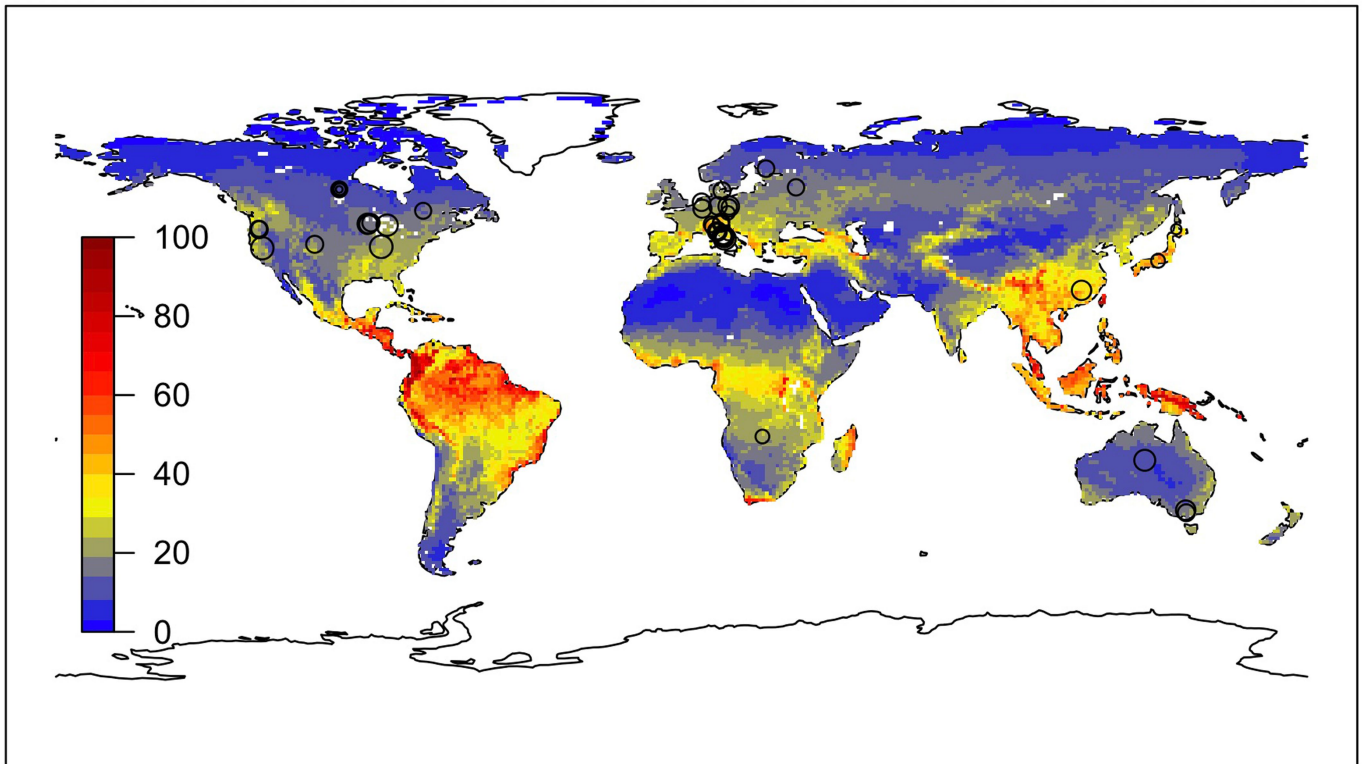
Extended Data Fig. 1 | Map of the included eddy covariance flux sites overlaid on species richness. Species richness is shown by different colours (data from http://ecotope.org/anthromes/biodiversity/plants/data/). Size of the circle is representative of the sample size of included days ranging from 10 (smallest circles) to 1,057 (largest circles) samples.
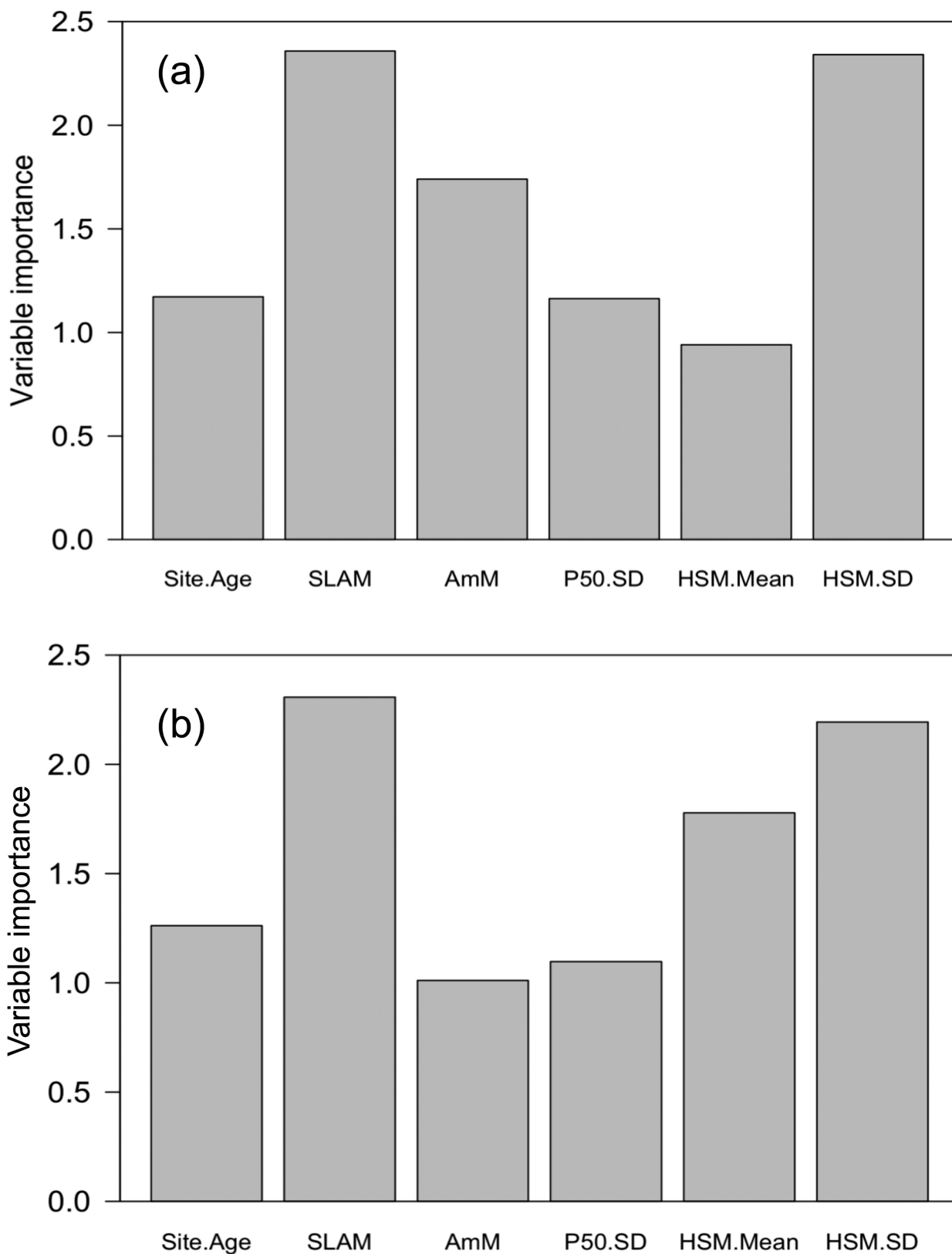
Extended Data Fig. 2 | Variable importance analysis for traits at flux sites. a, b, Variable importance (total decrease in node impurities) results from the machine-learning algorithm, random forests, for each variable for drought sensitivity (**a**) and drought coupling (**b**) metrics. Traits include SLA, (A_{max}), P_{50} and HSM. The suffix 'm' indicates the community-weighted mean; the suffix 'SD' indicates the community-weighted standard deviation. See Supplementary Table 3 for sample sizes.
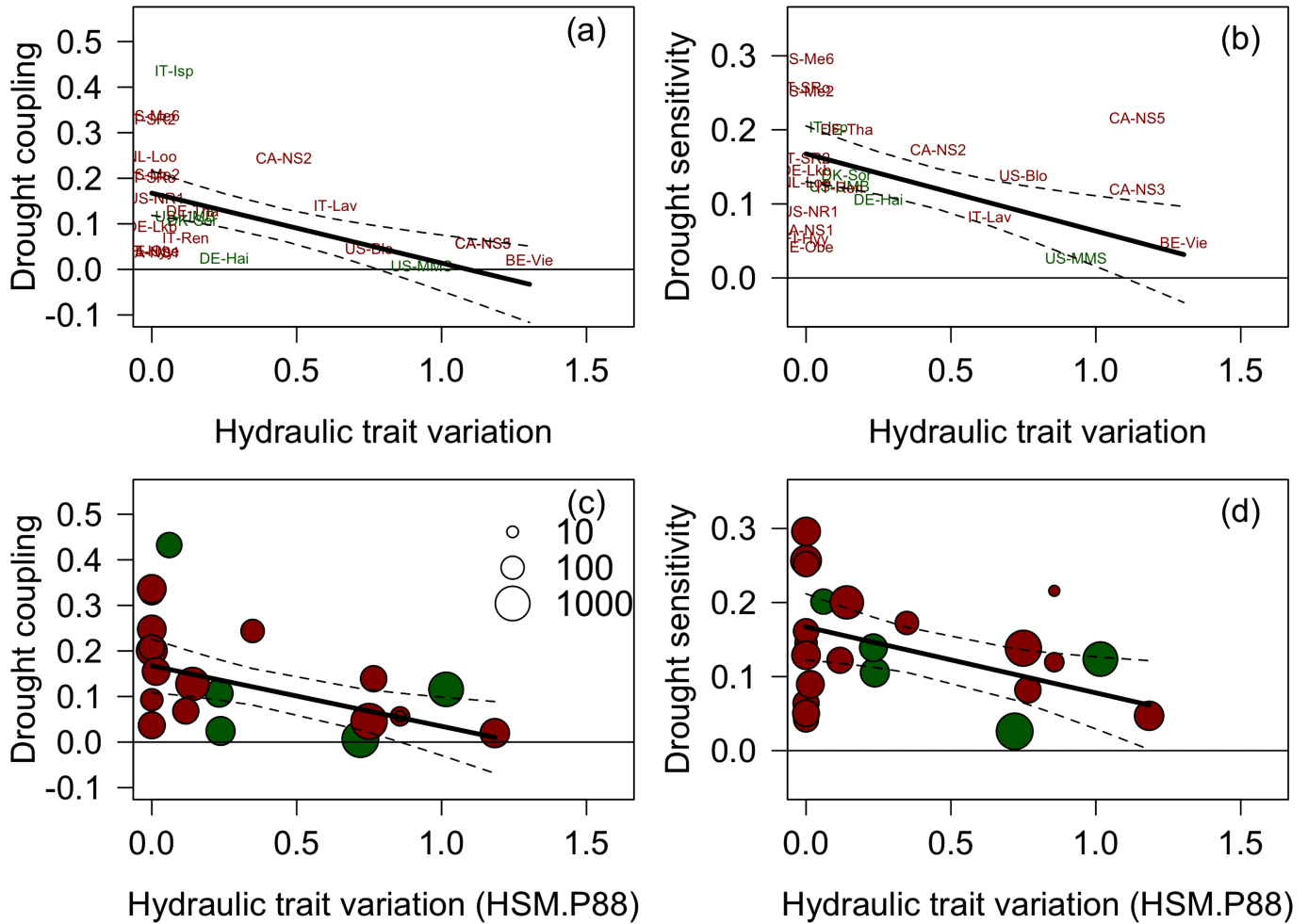
Extended Data Fig. 3 | Increased hydraulic variation buffers ecosystem drought responses. a, **c**, Drought coupling is expressed as the percentage of explained variation (R^2). **b**, **d**, Drought sensitivity is shown as the summed absolute values of standardized coefficients for drought variables that are regressed against latent energy (LE) exchange. Regression: LE ≈ VPD + SM + VPD × SM. **a**, **b**, Panels are identical to Fig. 2 but with site identifications shown. Hydraulic variation is expressed as the community-weighted standard deviation in the hydraulic safety margin of species. **c**, **d**, The hydraulic safety margin was calculated from the 50% loss of hydraulic conductivity in gymnosperms and 88% loss of hydraulic conductivity in angiosperms. Colours indicate biomes of deciduous broadleaf (green) and needleleaf (red) forests. The size of the dot indicates the number of days included for each flux site. The solid black line is the best fit of the ordinary least-squares linear regression (**c**, $P = 0.008$; **d**, $P = 0.01$) and dashed lines are the 95% confidence interval of the regression fit.
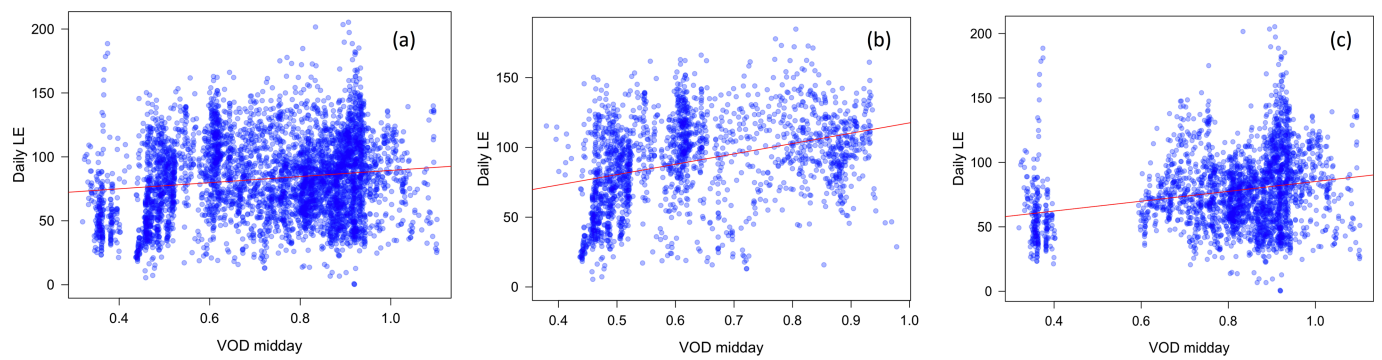
**Extended Data Fig. 4 | Satellite comparisons to flux towers.**
a–c, Relationship between daily total latent energy (LE) exchange measured via eddy covariance and midday canopy water content from remote-sensing of VOD for global forest sites (**a**; $n = 4,525$ grid cells), broadleaf forest sites (**b**; $n = 1,915$ grid cells) and evergreen forest sites (**c**; $n = 2,610$ grid cells). Red lines indicate best fits for ordinary least-squares regressions. Note that the canopy water content at each pixel integrates a spatial area that is two orders of magnitude greater than the eddy covariance sites.
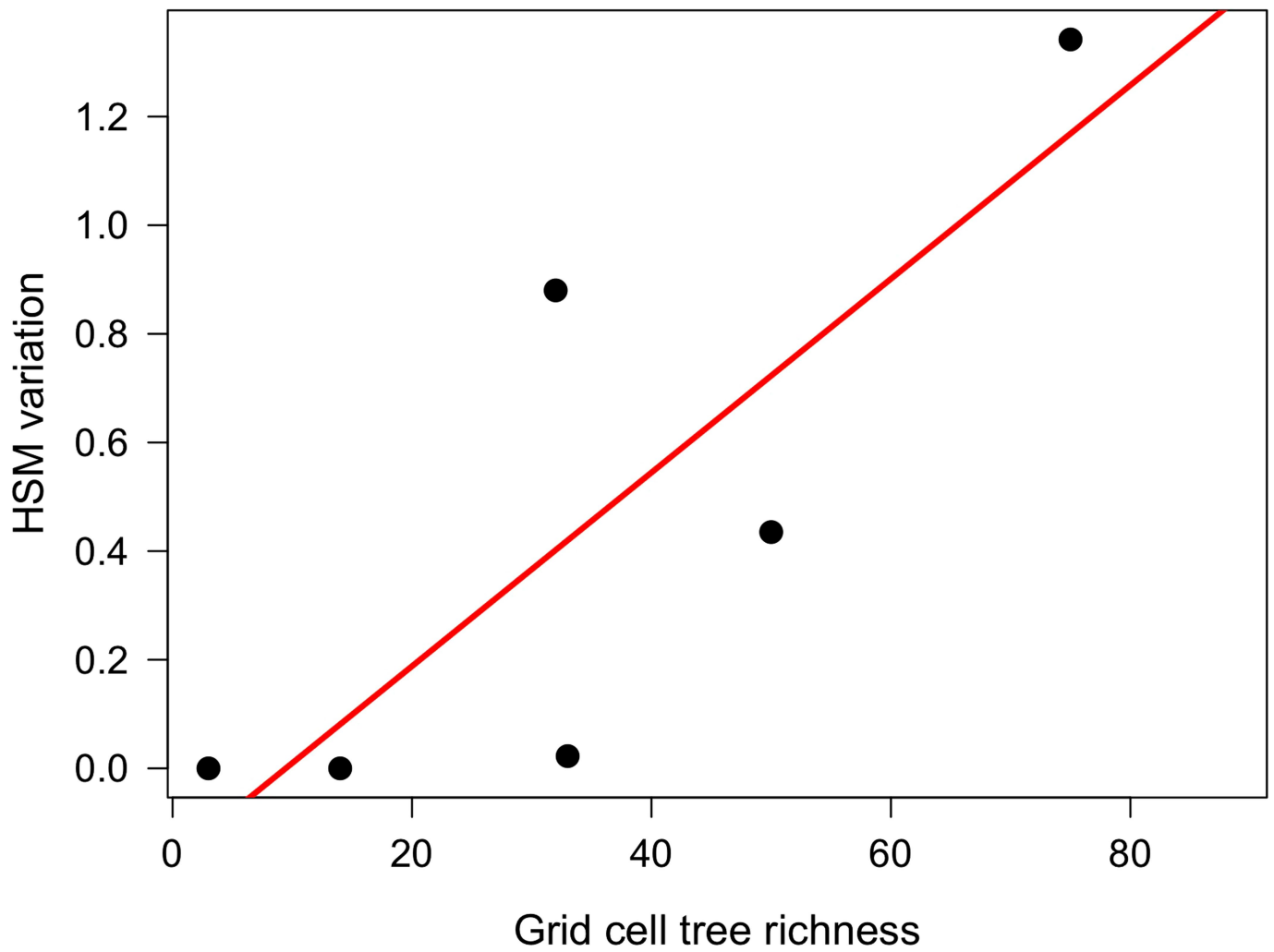
Extended Data Fig. 5 | Hydraulic trait variation compared to species richness. Comparison of dominant tree species richness from gridded data of US forests against the hydraulic diversity—the standard deviation in HSM—at six eddy covariance sites in the United States that have adequate trait data. The red line indicates the best fit of the ordinary least-squares linear regression ($n = 6$ sites; $R^2 = 0.65$; $P = 0.04$).
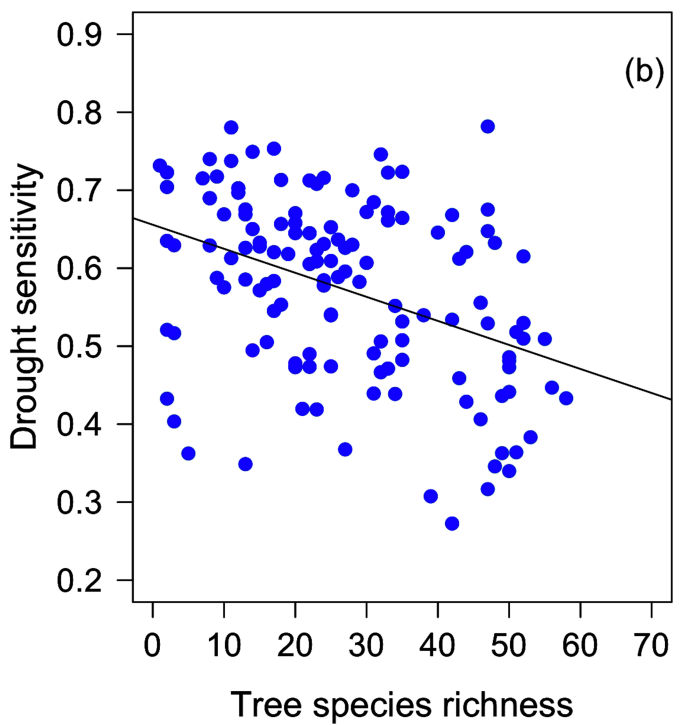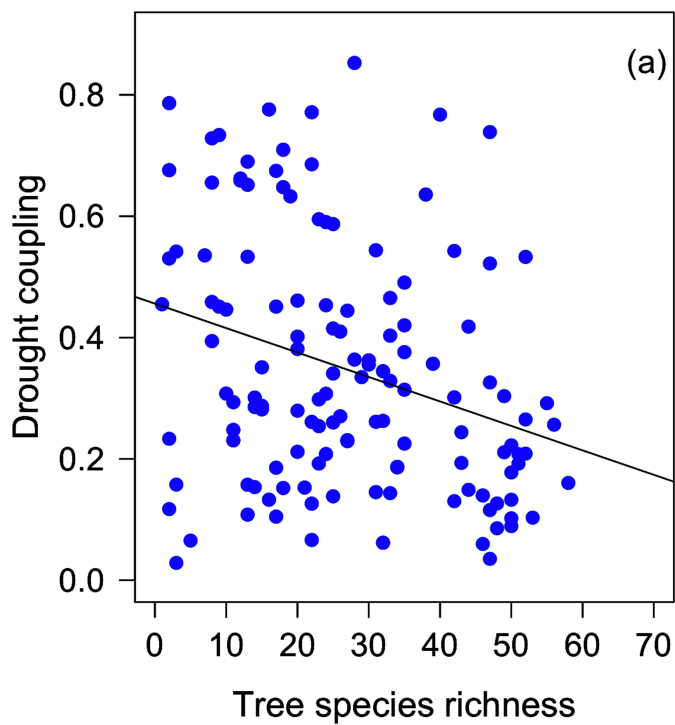
Extended Data Fig. 6 | Higher species diversity is associated with more buffered drought responses in US forests. a, b, Drought coupling (**a**; $n = 163$ grid cells) and drought sensitivity (**b**; $n = 163$ grid cells) from variation in remotely sensed canopy vegetation water content compared to tree species richness in the United States. Black line is the best fit of the ordinary least-squares linear regressions.
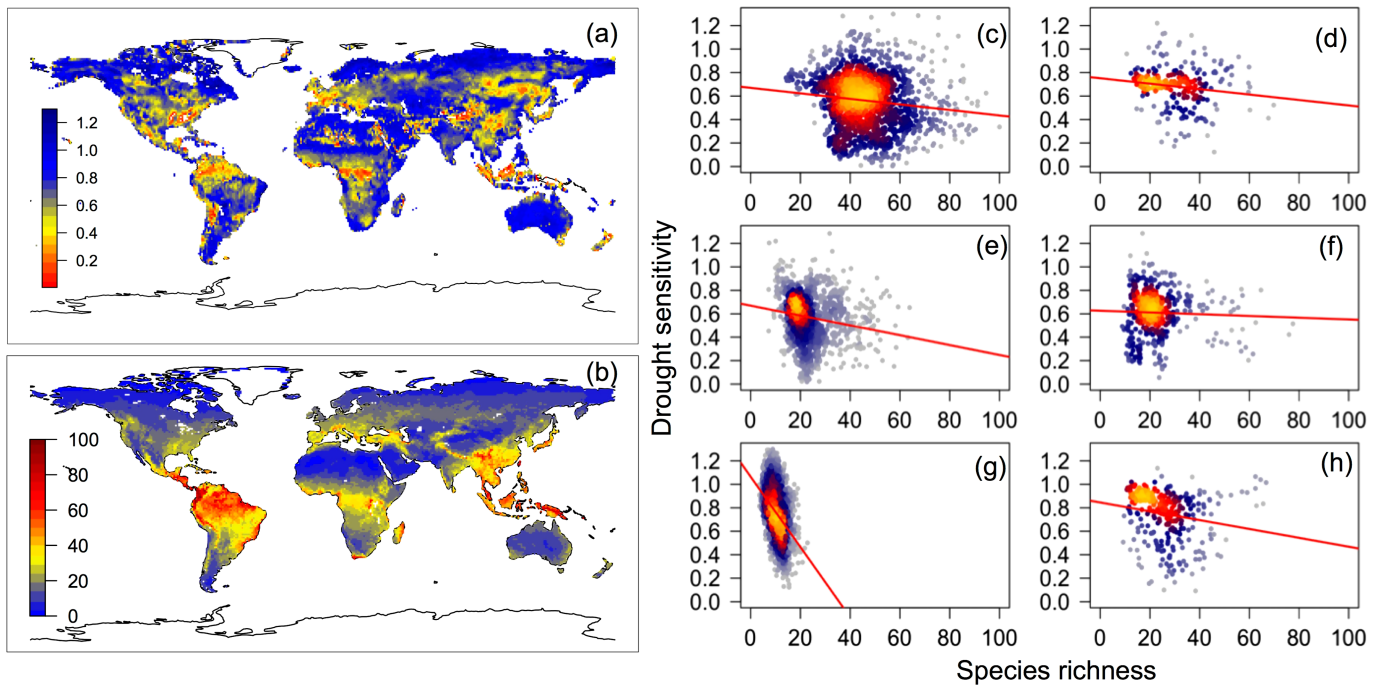
Extended Data Fig. 7 | Higher species diversity is associated with more-buffered drought responses in forests globally. a, Drought sensitivity as the slope (β) in an ordinary least-squares linear regression of an index of the variation in aboveground plant water content at midday compared to night (regression: $\mathrm{VOD_{midday}} = \beta \times \mathrm{VOD_{night}} + \varepsilon$). **b**, Native plant species richness (percentage of maximum; data from http://ecotope.org/anthromes/biodiversity/plants/data/). **c–h**, Ordinary least-squares linear regressions between these two variables for six major biomes. **c**, Tropical and subtropical moist broadleaf forests ($n = 1,380$ grid cells). **d**, Tropical and subtropical dry broadleaf forests ($n = 241$ grid cells). **e**, Temperate broadleaf and mixed forests ($n = 1,289$ grid cells). **f**, Temperate coniferous forests ($n = 318$ grid cells). **g**, Boreal forests ($n = 1,784$ grid cells). **h**, Mediterranean-type forests, woodlands and shrub ($n = 319$ grid cells). Each point represents an individual grid cell from the map and colours that are more red indicate a higher density of points. Red lines show the best fit of ordinary least-squares linear regression lines.
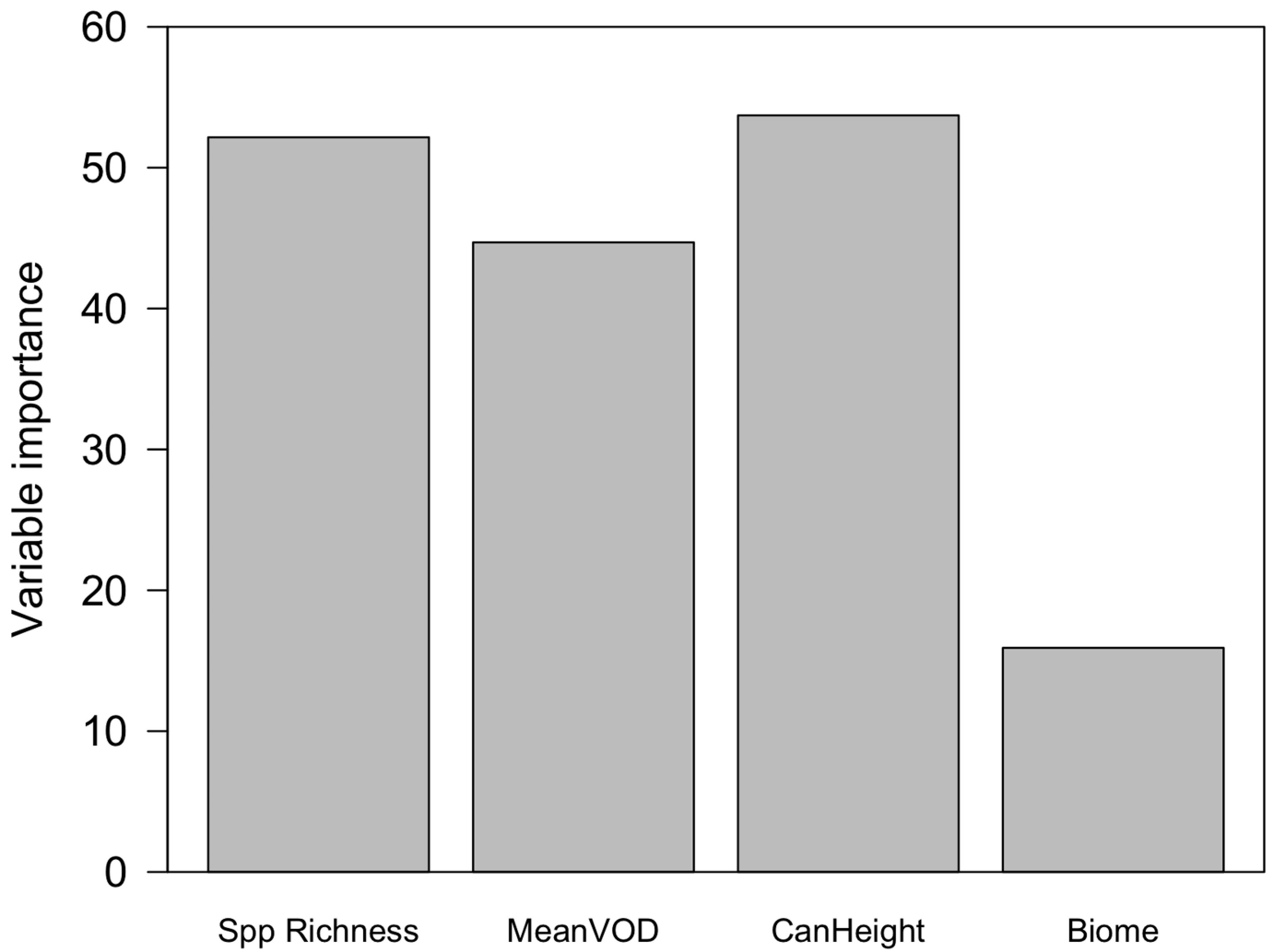
Extended Data Fig. 8 | Analyses of the importance of variables using satellite data. The importance of the variables (total decrease in node impurities) results obtained using the machine learning algorithm, random forests, for each variable of the drought coupling metric ($n = 6{,}698$ grid cells). 'CanHeight', lidar-derived canopy height.
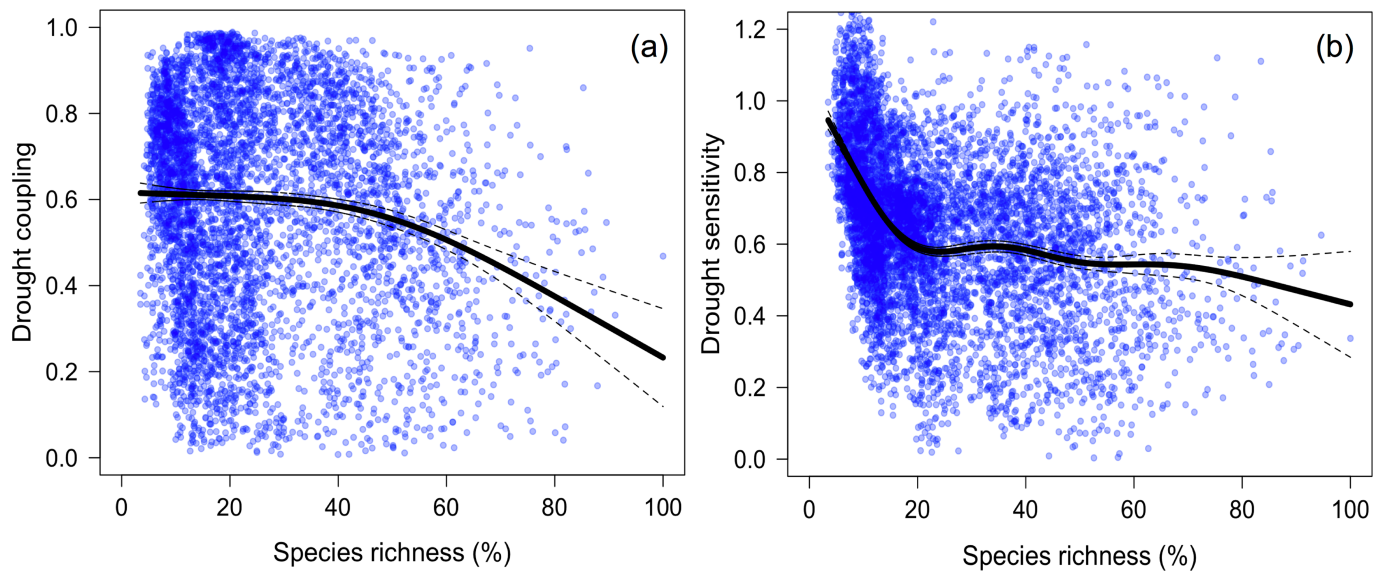
Extended Data Fig. 9 | Ecosystem sensitivity to drought saturates with species richness (the percentage of maximum) across forests globally. a, Drought coupling is expressed as the explained variation (R^2) of midday aboveground plant water content in forest ecosystems regressed against drought variables using ordinary least-squares linear regression.

b, Drought sensitivity is expressed as the regression coefficient of midday aboveground plant water content regressed against a metric of soil water stress using ordinary least-squares linear regression. $n = 6,698$ grid cells. The black line shows the best fit generalized additive model and dashed lines are the 99% confidence interval.
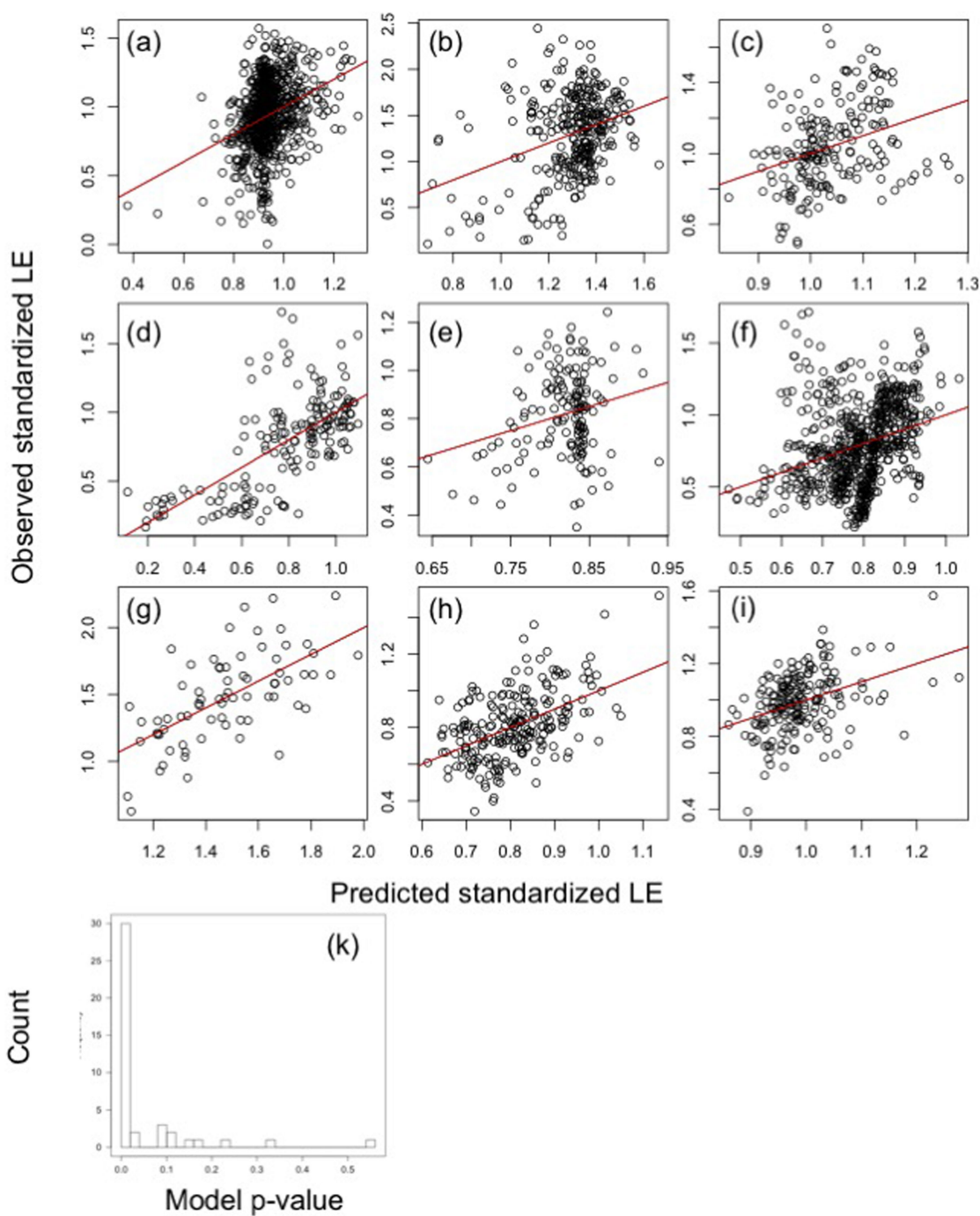
Extended Data Fig. 10 | Performance of the multivariate drought regression model. Nine randomly selected sites of observed latent energy (LE) fluxes versus predicted fluxes from the multiple regression model based on VPD, soil moisture and their interaction. Red lines are the ordinary least-squares best-fit regression line. Sites are as follows (abbreviations can be found in Supplementary Table 1). **a**, US-UMB ($R^2 = 0.12$, $P < 0.0001$). **b**, US-WCr ($R^2 = 0.13$, $P < 0.0001$). **c**, DK-Sor ($R^2 = 0.11$, $P < 0.0001$). **d**, IT-Ca1 ($R^2 = 0.44$, $P < 0.0001$). **e**, IT-PT1 ($R^2 = 0.06$, $P = 0.002$). **f**, IT-Ro1 ($R^2 = 0.10$, $P < 0.0001$). **g**, JP-SMF ($R^2 = 0.40$, $P < 0.0001$). **h**, NL-Loo ($R^2 = 0.25$, $P < 0.0001$). **i**, US-NWR ($R^2 = 0.15$, $P < 0.0001$). **k**, Performance of the drought multivariate ordinary least-squares linear regression model ($LE = f(VPD, SM, VPD \times SM)$) across eddy covariance sites shown in a histogram of site-level model P values from those regressions.

Corresponding author(s):   William Anderegg 2017-11-15274C

Reporting Summary

Nature Research wishes to improve the reproducibility of the work that we publish. This form provides structure for consistency and transparency in reporting. For further information on Nature Research policies, see Authors & Referees and the Editorial Policy Checklist.

Statistical parameters

When statistical analyses are reported, confirm that the following items are present in the relevant location (e.g. figure legend, table legend, main text, or Methods section).

n/a	Confirmed	
☐	☒	The exact sample size (*n*) for each experimental group/condition, given as a discrete number and unit of measurement
☐	☒	An indication of whether measurements were taken from distinct samples or whether the same sample was measured repeatedly
☐	☒	The statistical test(s) used AND whether they are one- or two-sided *Only common tests should be described solely by name; describe more complex techniques in the Methods section.*
☐	☒	A description of all covariates tested
☐	☒	A description of any assumptions or corrections, such as tests of normality and adjustment for multiple comparisons
☐	☒	A full description of the statistics including central tendency (e.g. means) or other basic estimates (e.g. regression coefficient) AND variation (e.g. standard deviation) or associated estimates of uncertainty (e.g. confidence intervals)
☐	☒	For null hypothesis testing, the test statistic (e.g. F, t, r) with confidence intervals, effect sizes, degrees of freedom and P value noted *Give P values as exact values whenever suitable.*
☒	☐	For Bayesian analysis, information on the choice of priors and Markov chain Monte Carlo settings
☒	☐	For hierarchical and complex designs, identification of the appropriate level for tests and full reporting of outcomes
☒	☐	Estimates of effect sizes (e.g. Cohen's *d*, Pearson's *r*), indicating how they were calculated
☐	☒	Clearly defined error bars *State explicitly what error bars represent (e.g. SD, SE, CI)*

Our web collection on statistics for biologists may be useful.

Software and code

Policy information about availability of computer code

Data collection	All analysis code is publicly available through the open-source R packages cited in the manuscript.
Data analysis	All analysis code is publicly available through the open-source R packages cited in the manuscript.

For manuscripts utilizing custom algorithms or software that are central to the research but not yet described in published literature, software must be made available to editors/reviewers upon request. We strongly encourage code deposition in a community repository (e.g. GitHub). See the Nature Research guidelines for submitting code & software for further information.

Data

Policy information about availability of data

All manuscripts must include a data availability statement. This statement should provide the following information, where applicable:

- Accession codes, unique identifiers, or web links for publicly available datasets
- A list of figures that have associated raw data
- A description of any restrictions on data availability

The FLUXNET2015 data is publicly available at http://fluxnet.fluxdata.org/data/fluxnet2015-dataset/

Field-specific reporting

Please select the best fit for your research. If you are not sure, read the appropriate sections before making your selection.

☐ Life sciences ☐ Behavioural & social sciences ☒ Ecological, evolutionary & environmental sciences

For a reference copy of the document with all sections, see nature.com/authors/policies/ReportingSummary-flat.pdf

Ecological, evolutionary & environmental sciences study design

All studies must disclose on these points even when the disclosure is negative.

Study description	Analysis of publicly available eddy covariance data with publicly available trait data.
Research sample	Meteorological measurements and eddy covariance measurements of latent energy exchange from the publicly available FLUXNET2015 dataset.
Sampling strategy	n/a
Data collection	n/a
Timing and spatial scale	n/a
Data exclusions	n/a
Reproducibility	n/a
Randomization	n/a
Blinding	n/a

Did the study involve field work? ☐ Yes ☒ No

Reporting for specific materials, systems and methods

Materials & experimental systems

n/a	Involved in the study
☒	☐ Unique biological materials
☒	☐ Antibodies
☒	☐ Eukaryotic cell lines
☒	☐ Palaeontology
☒	☐ Animals and other organisms
☒	☐ Human research participants

Methods

n/a	Involved in the study
☒	☐ ChIP-seq
☒	☐ Flow cytometry
☒	☐ MRI-based neuroimaging